JOURNAL OF MATERIALS SCIENCE **34** (1999) 645–651

Effect of prior cold rolling and test temperature on stress-strain rate behaviour of a Zr-2.5Nb alloy

B. P. KASHYAP, R. PATHAK*, K. NARASIMHAN
Department of Metallurgical Engineering and Materials Science, Indian Institute of Technology, Bombay, Mumbai 400 076, India
E-mail: bpk@met.iitb.ernet.in

R. KISHORE, R. K. FOTEDAR, T. K. SINHA
Metallurgy Division, Bhabha Atomic Research Centre, Mumbai 400 085, India

Zr-2.5 wt % Nb alloy sheet, obtained by unfolding and straightening a pressure tube, was further cold rolled upto 39% reduction in thickness to investigate the effect of cold working on the stress (σ)-strain rate ($\dot{\varepsilon}$) behaviour over a strain rate range of $\sim 2 \times 10^{-5}$ to 5×10^{-3} s^{-1} and a temperature range of 625 to 700 °C. Irrespective of the amount of rolling, the log σ vs log $\dot{\varepsilon}$ plots exhibit superplastic behaviour with strain rate sensitivity index, m, as high as 0.8, which decreases to 0.2 at higher strain rates. On the other hand, the activation energy for deformation, Q, increases from 171.1 kJ/mol for superplastic deformation to 249 kJ/mol in Region III. The tendency for improved superplasticity (m) is seen upon cold working by 22% or more at the test temperatures 675 and 700 °C.

1. Introduction

Superplasticity, the ability of certain materials to deform to the ductility of several hundred percent, is exhibited during uniaxial tensile test at high temperatures and intermediate strain rates, in the presence of fine equiaxed grains [1]. The flow stress, σ, vs strain rate, $\dot{\varepsilon}$, plot in log-log scale shows a sigmoidal curve having three regions with the slope, called strain rate sensitivity index, m, being greater than 0.3 in the intermediate strain rate range. This is known as superplastic region or Region II. At lower (Region I) as well as higher (Region III) strain rates, m is less than 0.3. The superplastic region shifts towards higher strain rates with the decrease in grain size. Positive exponent superplasticity, whereby superplasticity prevails close to commercial hot working rates ($\dot{\varepsilon} \sim 10^{-1}$ to 10 s^{-1}), was reported recently in nano or near-nano scale aluminium alloys [2]. Ductility increases with the decrease in grain size [1] and increase in strain rate sensitivity index [3].

The conventional method of grain refinement involves heavy cold working and annealing for recrystallization or hot working for dynamic recrystallization. Fabrication of Zr-2.5 wt % Nb alloy (hereafter referred as Zr-2.5Nb) for pressure tubes in the pressurized heavy water reactors involves both the hot and cold working [4]. This gives strongly textured two-phase structure with the β-Zr phase stringers distributed along the boundaries of the elongated α-Zr grains. While this structure contributes to strengthening and creep resistance during service at temperatures around 300 °C in the reactors [5], the fine equiaxed grains are developed, leading to poor creep properties, at temperatures in the α-β two-phase region. In fact, such microstructures are suitable for superplasticity, and a maximum ductility exceeding 650% is reported [6]. The aim of the present work is to find the effect of prior cold working and test temperature on the nature of σ-$\dot{\varepsilon}$ curves for the Zr-2.5Nb alloy, so as to identify the conditions for the maximum m, which proportionately relates to the ductility maxima.

2. Experimental

The Zr-2.5Nb alloy, with chemical composition (wt %): 2.54 Nb, 0.1175 O and balance Zr, was obtained in the cold worked and stress-relieved state [4] in the form of 4 mm thick sheet, after cutting and straightening from the pressure tubes. These sheets were further rolled at room temperature to 0, 12, 22 and 39% reduction in thickness, designated as A-R, R-I, R-II and R-III, respectively. Then the pieces for metallographic and tensile samples were cut. The tensile samples were machined to get a gauge length of 12.7 mm and a gauge width of 4.3 mm.

Metallographic samples were mechanically polished and etched with HNO_3 : HF : H_2O in a proportion of 45 : 5 : 50. The grain size ($d = 1.74 \times$ mean intercept length) was measured from the scanning electron micrographs, with no distinction being made between the α and β phases. The average grain sizes reported here are based on counting more than 500 intercepts for each d, with errors within $\pm 10\%$ at a confidence level of 95%.

Tensile specimens were coated with borosilicate glass powder and the tests were done in argon

* *Present address:* Sunflag Iron & Steel Co. Ltd., Bhandara 441 905, India.

atmosphere in order to avoid oxidation. Tensile tests were conducted with Instron Universal testing machine by employing differential strain rate test technique. In this technique, the same specimen is deformed at various strain rates instead of deforming separate specimens at each strain rate. The change in strain rate in differential strain rate test technique is made when the flow stress tends to approach steady state i.e., it becomes reasonably independent of strain, during deformation at the current strain rate (cross-head speed). Thus, a large number of stress-strain rate data can be obtained from a single specimen, which eliminates the effect of variation from sample to sample. The test temperatures were controlled within $\pm 2\,^{\circ}$C, and it took an hour for heating to and soaking at the first test temperature, prior to straining. After completing the differential strain rate test of one cycle at the selected temperature, the test temperature was changed to another value at which 15 min were allowed for stabilizing. The stress-strain rate data, collected from low towards high strain rates, at each temperature is designated by a cycle number. The first cycle of data was obtained at 650 °C whereas the increasing cycle numbers correspond to the subsequently changed temperatures as per a selected sequence.

3. Results

Metallographic samples of the as-received as well as of the subsequently rolled sheets exhibited very fine elongated microstructures, which coarsened with a simultaneous reduction in the grain aspect ratio during short time annealing. This aspect is described elsewhere [7]. The grain sizes, just before starting the tensile test for the first cycle, were obtained from the metallographic specimens put alongwith the tensile specimens but quenched after the heating and soaking time only. These grain sizes were measured to be 2.7, 3.8, 2.2 and 2.2 μm for 0, 12%, 22% and 39% rolled sheets, respectively.

Tensile specimens machined from the sheets, after different amount of rolling, were deformed over the strain rate range of $\sim 2 \times 10^{-5}$ to 5×10^{-3} s^{-1} and the temperature range of 625 to 700 °C. All the specimens were first deformed at 650 °C because the maximum ductility was reported [6] at this temperature. The same specimens were then deformed at 700 °C, the highest test temperature, for stabilizing the microstructure, and the tests were subsequently continued at lower temperatures, viz. 675, 625 and 650 °C. Thus the σ-$\dot{\varepsilon}$ data corresponding to 650, 700, 675, 625 and 650 °C are designated as cycles I, II, III, IV and V, respectively. The final differential strain rate test at 650 °C was conducted to study the effect of intermediate deformation, at other temperatures, on the nature of σ-$\dot{\varepsilon}$ plot by comparing the data from I and V cycles. Described below is the deformation behaviour.

3.1. Stress-strain rate behaviour

Fig. 1(a–d) shows the five cycles of log σ vs log $\dot{\varepsilon}$ plots, with each cycle of the data collected at new test temperatures. Irrespective of the amount of prior cold working, log σ vs log $\dot{\varepsilon}$ curves depict two regimes – comprising of typical superplastic region with a higher slope at lower strain rates (Region II), and a non-superplastic region with lower slope (Region III) at the higher strain rates. As expected, the flow stresses at the highest test temperature, viz. 700 °C are found to be the minimum and that at the lowest test temperature of 625 °C to be the maximum. However, the flow stress obtained from the last cycle (cycle V) has changed in comparison to the first cycle data at the same test temperature of 650 °C. At lower strain rates the flow stress from the last cycle is noted to be higher than that from the first cycle whereas the reverse is true at higher strain rates.

TABLE I Variation in m with test temperature and degree of cold rolling (m in Regions II and III obtained from regression lines with r better than 0.90)

Degree of cold rolling (% reduction in thickness)		Test temperature (°C) 650(I)	700	675	625	650(II)
		Region II				
AR	(0)	0.51	0.47	0.44	0.29	0.37
R-I	(12)	0.46	0.60	0.49	0.34	0.41
R-II	(22)	0.61	0.71	0.70	0.46	0.57
R-III	(39)	0.57	0.69	0.76	0.39	0.50
		Region III				
AR	(0)	0.24	0.27	0.25	0.17	0.21
R-I	(12)	0.23	0.29	0.23	0.17	0.18
R-II	(22)	0.30	—	0.30	0.18	0.19
R-III	(39)	0.26	0.36	0.30	0.18	0.18

Strain rate sensitivity index, m, was calculated by two methods: (i) From the load-elongation curves according to Backofen's method [8] – m values are plotted as a function of log $\dot{\varepsilon}$ in Fig. 2(a–d). (ii) From the slope of the log σ vs log $\dot{\varepsilon}$ plots – the data points in Regions II and III, Fig. 1, suggest single straight lines in each region. Presented in Table I are the m values based on regression analysis in each region, with the correlation coefficient, r, better than 0.90. From Fig. 2, it seems that m is improved upon rolling, with the effect being more as the test temperature increases. At all the test temperatures and rolling conditions, m decreases with increasing strain rate but tends to approach a plateau towards the higher strain rates. Although the effect of rolling and test temperature is not very clear from Table I, it appears to suggest that m is larger for R-II and R-III conditions and, as far as the effect of temperature is concerned, the lower values of m are noted at 625 °C. On comparing m vs log $\dot{\varepsilon}$ plots for cycles I and V at 650 °C, m is noted to be lowered by the deformation introduced during the intermediate cycles of the σ-$\dot{\varepsilon}$ data.

3.2. Effect of temperature

With the increase in test temperature, the flow stress at constant strain rate decreases whereas the strain rate at a fixed stress increases. Arrhenius plots, Fig. 3(a, b), were made to calculate activation energies, Q, for deformation in Region II and Region III at constant strain rates of 1×10^{-4} and 2×10^{-3} s^{-1}, respectively. The equation employed can be written as

$$Q = R/m\,[\delta \ln \sigma / \delta(1/T)]_{\dot{\varepsilon},d}$$

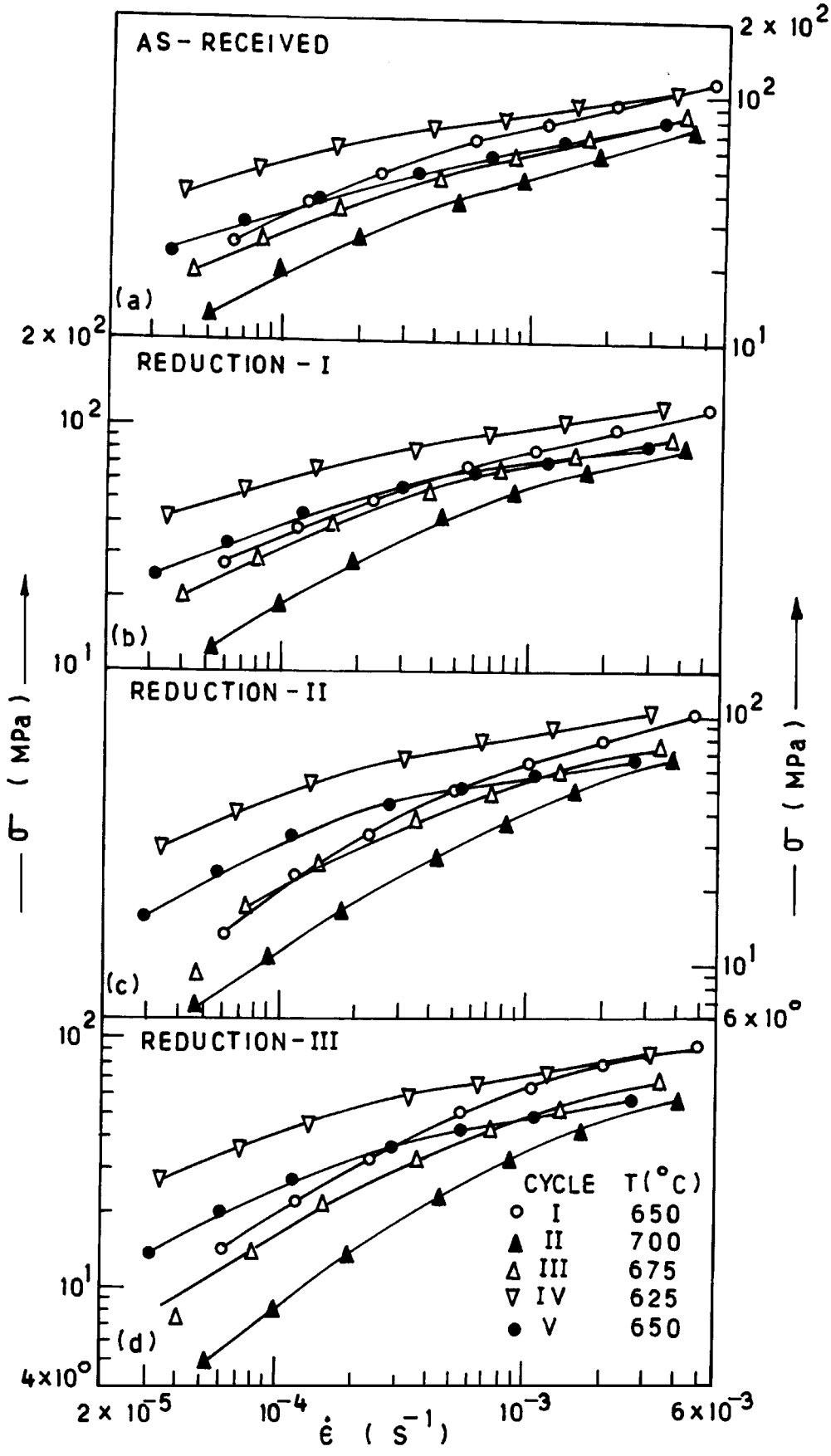

Figure 1 Log σ vs log $\dot{\varepsilon}$ plots over the temperature range of 625 to 700 °C for the Zr-2.5Nb alloy cold rolled to varying degree: (a) 0% (as-received), (b) 12% (R-I), (c) 22% (R-II) and (d) 39% (R-III).

where R and T have their usual meanings and the other terms are already defined. For this purpose, the average values of m were taken at the selected strain rates and for each rolling condition from Fig. 2. The last cycle of the σ-$\dot{\varepsilon}$ data at 650 °C was not considered in view of the observed effect of the accumulated strain, Fig. 1. Also, the data at 625 °C in Region II were excluded as this region is not developed adequately.

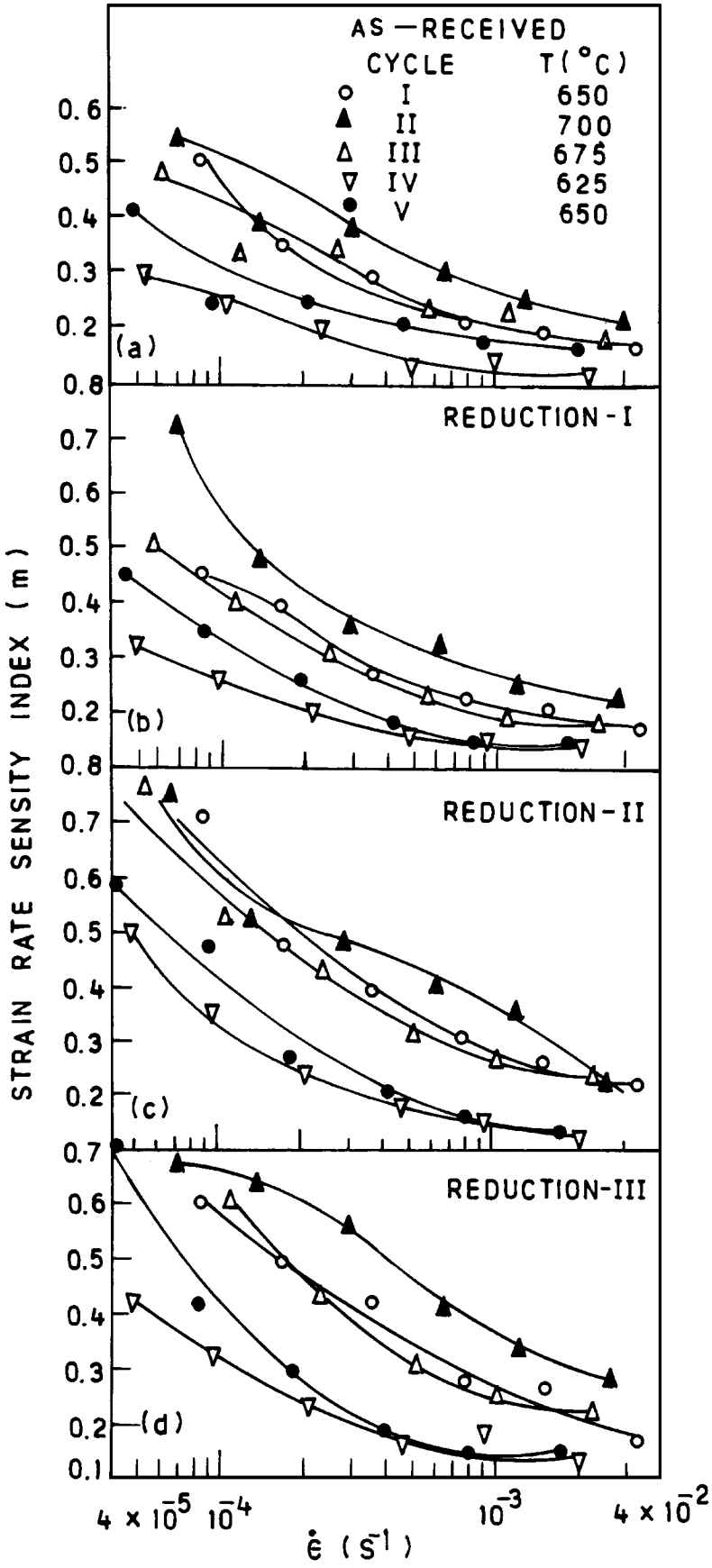

Figure 2 m vs log $\dot{\varepsilon}$ plots over the temperature range of 625 to 700 °C for the Zr-2.5Nb alloy cold rolled to varying degree: (a) 0% (as-received), (b) 12% (R-I), (c) 22% (R-II) and (d) 39% (R-III).

The values of Q in Regions II and III are listed in Table II. There does not appear any systematic effect of prior cold rolling on the Q values. The average values of Q in Regions II and III are determined to be 171.1 and 249.0 kJ/mol, respectively.

3.3. Microstructural evolution

Upon completion of the last cycle of differential strain rate test, each specimen was rapidly cooled by removing from the test assembly and quenching in water. Metallographic specimens were prepared from the shoulder

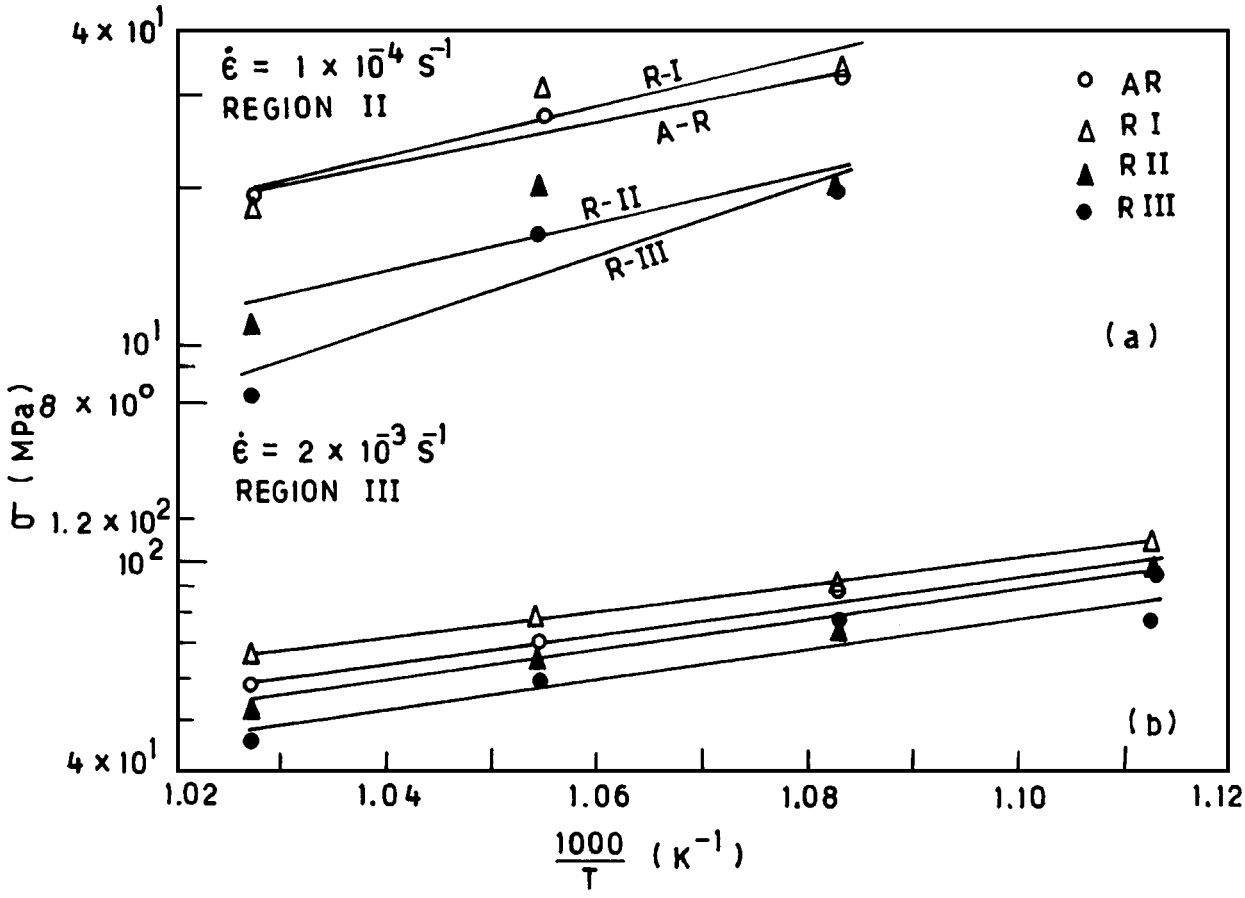

Figure 3 Arrhenius plots for determination of activation energy for deformation in: (a) Region II and (b) Region III.

TABLE II Values of activation energy, Q, in Regions II and III for the samples undergone different degree of cold rolling

Degree of cold rolling (% reduction in thickness)			Q (kJ/mol)	
			Region II	Region III
AR	(0)		158.3	262.9
R-I	(12)		185.7	241.5
R-II	(22)		137.1	248.4
R-III	(39)		203.4	243.2
		Average	171.1	249.0

and gauge sections of each specimen. The microstructures in the gauge sections were equiaxed and slightly coarser than those in the shoulder sections, which exhibited elongated grains. The microstructures of the specimens with different amount of cold rolling were found to be similar. Fig. 4(a, b) illustrates the microstructures obtained in the shoulder and gauge sections of the tensile specimen prepared from the R-II sheet. The grain size of 2.7 μm, calculated as an average for all the prior cold worked conditions, at the start of the test, changed to 2.8 μm in the shoulder section and 3.1 μm in the gauge section upon completion of the tests.

4. Discussion

The log σ vs log $\dot{\varepsilon}$ plots for all the amount of cold rolling, Fig. 1, exhibit similar behaviour with two regimes. The absence of any significant effect of cold rolling is noted in the microstructures developed during heating and soaking of the tensile specimens prior to straining, so also subsequent to tensile tests. As the cold worked materials undergo recovery, recrystallization and grain growth during heating and soaking prior to tensile test, the substructural changes associated with the first two steps depend on the amount of cold rolling. Whereas the absolute value of the stored energy generally increases as the strain increases, it reaches a limiting value in some polycrystalline metals [9, 10]. The comparable grain sizes and the similar nature of the log σ vs log $\dot{\varepsilon}$ curves for the different amount of prior cold rolling, therefore, may be the result of such a limiting value of stored energy attained in the as-received Zr-2.5Nb alloy.

The log σ vs log $\dot{\varepsilon}$ curves at 650 °C for the I cycle and V cycle cross-over each other at intermediate strain rates. The difference between the two curves should be related to the difference in the microstructures in the beginning of the test and at the end of the test. The noticeable difference here is the change in grain morphology from elongated to equiaxed, whereas grain growth is only marginal (i.e., 2.7 μm became 3.1 μm). In several other materials, it is known [11, 12] that the change in grain shape, from the initially elongated to equiaxed, leads to strain softening. The σ-$\dot{\varepsilon}$ data in Fig. 1 exhibits such a lowering of flow stress only towards higher strain rates. The increase in flow stress is attributed [11, 12] to grain growth but the reasonably stable grain sizes noted here do not suggest this to be a possibility for the higher flow stress of cycle V towards lower strain rates. This was checked by calculating the flow stress

TABLE III Values of activation energy for diffusion in Zr, Nb, and Zr-Nb alloys

Process	Material	Range of temp. (°C)	Q (kJ/mol)	Remark	Ref.
Lattice self diffusion	β-Zr	900–1750	116.1/273.2	log D vs 1/T curved	[15]
	Nb	1080–2420	349.9/438.7	— do —	[15]
Tracer impurity diffusion	^{95}Zr in Nb	1582–2084	364.5		[15]
	^{95}Nb in Zr	740–857	132.0		[15]
		(α-Zr)	105.2 + 148.7		[15]
		880–1750 (β-Zr)	(T-1136)		[15]
Homogeneous alloys	Zr-2.3Nb	900–1160	162.6	^{95}Nb diffusion	[15]
	Zr-5Nb	1200–1500	209.5/169.7	Q_{Nb}/Q_{Zr}	[15]
	Zr-10Nb	1200–1500	230.5/196.9	— do —	[15]
	Zr-15Nb	1200–1500	243.0/211.6	— do —	[15]
Chemical diffusion	Zr-Nb of various compositions	900–1600	217.9 to 333.1	Increases as Nb increases from 5 at % to 95 at %	[15]
	Zr-Nb alloys including pure metals	1445–1690	196.9(Zr) 389.7 (Nb)	Increases as Nb increases from 0 to 100 at %	[15]
^{95}Nb diffusion along the α/β interphase boundaries	Zr-2.5Nb	702–818	105/230	Q increases with temperature	[16]
		715–818	288	Recalculated from Ref. (16)	[17]
^{95}Zr diffusion along the α/β interphase boundaries	Zr-2.5Nb	649–836	306		[18]
High temp. deformation	Zr-2.5Nb	650–700	171.1	Superplasticity	Present work
		625–700	249.0	Region III	— do —

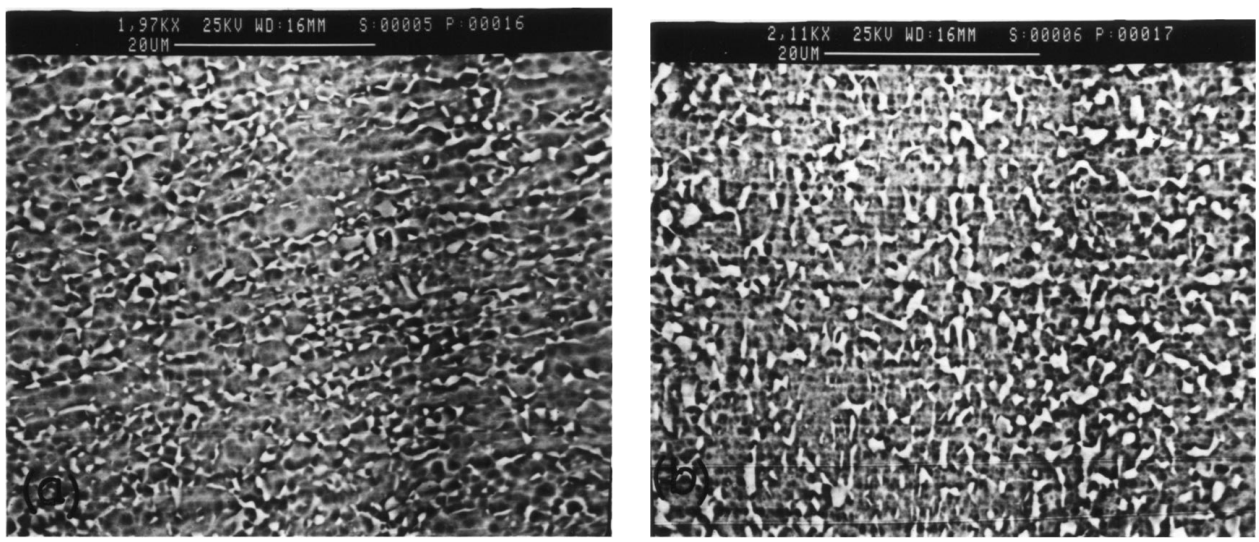

(a) (b)

Figure 4 Typical microstructures developed in the shoulder (a) and gauge (b) sections of the tensile specimens in the course of differential strain rate tests. (R-II, i.e. 22% cold rolled).

on the basis of instantaneous grain size and using the relationship $\sigma \alpha d^{p.m}$ for both the first and the last cycle data. Here the grain size exponent known for superplastic deformation ($p = 2$–3) was used. Whether there is an increase in dislocation density to account for the increase in flow stress or there occurs cavitation to account for strain softening need to be examined. Our preliminary examination of the deformed specimens for cavitation did not reveal cavities except on the fracture surfaces.

In Region II, m is greater than 0.3, which is well known for the superplastic materials. However, whether m remains constant over the entire Region II or it gradually increases with strain rate, reaching a maximum value, then decreases again is not universally accepted [1]. There are as many cases for the first trend as there exist for the second case. It appears from Fig. 1 that, whereas m in Regions II and III may be independent of strain rate, the transition between the two regions is gradual, which can contribute to its strain rate dependency. While the various models for superplastic deformation [13] suggest m to be constant at the value of 0.5, the Ashby-Verrall model [14] supports the continuous variation in m with strain rate. The activation energy for superplastic deformation is considered to compare with that for grain boundary diffusion in general. The present value of 171.1 kJ/mol, on the other hand, is comparable with the activation energy for lattice diffusion of Nb in Zr-2.3Nb alloy (162.6 kJ/mol) [15]. The relevant activation energies for the various

diffusional processes are presented from literature in Table III. The data for grain boundary diffusion are not available but the activation energy for diffusion along the α/β interphase boundary [16–18] is much larger. Thus, superplastic deformation in the Zr-2.5Nb alloy is suggested to occur by grain boundary sliding and its accommodation by diffusion of Nb atoms in the lattice.

In Region III, m is found to be less than 0.3 but the stress exponents ($n = 1/m$), in the relationship $\dot{\varepsilon} \alpha \sigma^n \exp(-Q/RT)$, during the first three cycles are lower (average $n = 3.6$) than that estimated during the last two cycles (average $n = 5.5$). However, all these values are closer to the predictions of the dislocation creep models ($n = 4.5$), which suggest the dislocation climb to be the rate controlling [16]. The activation energy for deformation of the present alloy (249 kJ/mol) compares with that for lattice diffusion of Nb in Zr-15Nb alloy (243 kJ/mol) [15]. The similarity between these two activation energies can be understood by the fact that the Zr-2.5Nb alloy, as obtained from the phase diagram [15], contains 10–19% β-phase having Nb from 18.5 to 11.1 wt % as the temperature increases from 625 to 700 °C. Thus, both the stress sensitivity and activation energy values suggest the deformation in Region III to be controlled by dislocation climb process.

5. Conclusions

The Zr-2.5Nb pressure tube material exhibits the maximum tendency for superplasticity, in terms of m values, at 675 and 700 °C when undergone additional cold working of 22% or more. The log σ vs log $\dot{\varepsilon}$ plots delineate two regions over $\dot{\varepsilon} \sim 2 \times 10^{-5}$ to 5×10^{-3} s^{-1} with the superplastic behaviour at lower strain rates and Region III behaviour towards higher strain rates. Over the investigated range of temperatures (625–700 °C), m decreases with the increase in strain rate from the maximum of ~0.8 in Region II to ~0.2 in Region III. The activation energy for deformation are estimated to be 171.1 kJ/mol and 249 kJ/mol, respectively.

Acknowledgements

This work was financially supported and permitted for publication by the Board of Research in Nuclear Sciences of India under grant no. 34/8/93-G/429. The authors are grateful to Dr. S. Banerjee for useful discussion and help throughout the period of this project.

References

1. K. A. PADMANABHAN and G. J. DAVIES, "Superplasticity" (Springer-Verlag, Berlin, 1980).
2. K. HIGASHI, in "Superplasticity: 60 years after Pearson" edited by N. RIDLEY (The Institute of Materials, London, 1995) p. 93.
3. D. A. WOODFORD, *Trans. ASM* **62** (1969) 291.
4. A. J. HAQ, A. HAQ and S. BANERJEE, *Bull. Mater. Sci.* **15** (1992) 289.
5. P. RODRIGUEZ, in Proc. Symp. on Zirconium Alloys for Reactor Components, ZARC-91 (Board of Research in Nuclear Sciences, Department of Atomic Energy of India, Bhabha Atomic Research Centre, Bombay, 1991) p. 46.
6. R. N. SINGH, R. KISHORE, T. K. SINHA and B. P. KASHYAP, *Scr. Metall. Mater.* **28** (1993) 937.
7. B. P. KASHYAP, R. PATHAK, R. KISHORE, R. K. FOTEDAR and T. K. SINHA, *Z. Metallkd.* **89** (1998) 303.
8. W. A. BACKOFEN, I. R. TURNER and D. H. AVERY, *Trans. ASM* **57** (1964) 980.
9. J. H. SMITH and M. B. BEVER, *Trans. Met. Soc. AIME* **242** (1968) 880.
10. R. O. WILLIAMS, *ibid.* **224** (1962) 719.
11. M. SUERY and B. BAUDELET, *Rev. Phys. Appl.* **13** (1978) 53.
12. B. P. KASHYAP, A. ARIELI and A. K. MUKHERJEE, *J. Mater. Sci.* **20** (1985) 2661.
13. B. P. KASHYAP and A. K. MUKHERJEE, in "Superplasticity," edited by B. BAUDELET and M. SUÉRY (C. N. R. S., Paris, 1985) p. 4.1.
14. M. F. ASHBY and R. A. VERRALL, *Acta Metall.* **21** (1973) 149.
15. E. A. BRANDES (Ed.,) "Smithells Metals reference book," 6th ed. (Butterworths, London, 1983) chapt. 13 and 11 p. 374.
16. R. PIOTRKOWSKI and F. DYMENT, *J. Nucl. Mater.* **137** (1986) 94.
17. R. PIOTRKOWSKI, *ibid.* **183** (1991) 221.
18. M. J. IRIBARREN and F. DYMENT, *ibid.* **161** (1989) 148.
19. J. CADEK, "Creep in Metallic Materials" (Elsevier and Academia, Chechoslovak Academy of Sciences, Prague, 1988) p. 115.

Received 1 June
and accepted 2 October 1998